Biochemical Engineering Journal 112 (2016) 32–41

Contents lists available at ScienceDirect

Biochemical Engineering Journal

journal homepage: www.elsevier.com/locate/bej

Regular article

Design and preparation of chimeric hyaluronidase as a chaperone for the subcutaneous administration of biopharmaceuticals

Shan Liu [a,b,1], Bo Xie [a,1], Wei Wei [a], Mizhou Hui [a,*], Zhiguo Su [a,c,*]

[a] National Key Laboratory of Biochemical Engineering, Institute of Process Engineering, Chinese Academy of Sciences, Beijing 100190, PR China
[b] University of Chinese Academy of Sciences, Beijing 100049, PR China
[c] Jiangsu National Synergetic Innovation Center for Advanced Materials (SICAM), Nanjing 210009, PR China

ARTICLE INFO

Article history:
Received 13 December 2015
Received in revised form 6 March 2016
Accepted 28 March 2016
Available online 30 March 2016

Keywords:
Recombinant DNA
Fed-batch culture
Purification
Biomedical
Long-acting hyaluronidase
Subcutaneous administration

ABSTRACT

Subcutaneous (SC) delivery of biomacromolecular pharmaceuticals such as proteins often encounter barriers in the extracellular matrix, especially the hyaluronan (HA) network. In this study, chimeric hyaluronidases were designed, prepared and tested for assisting biopharmaceuticals in ID administration in mice as replacement of SC administration. The chimeras were hyaluronidase (rhPH20) conjugated with human serum albumin (rhPH20-HSA) and antibody Fc fragment (rhPH20-Fc). Expression of the new protein was undertaken in CHO cells cultured in a 5-L disposable bioreactor. Purification was carried out by a series of chromatographic methods to obtain high-purity products of 61 kDa (rhPH20), 79 kDa (rhPH20-HSA) and 190 kDa (rhPH20-Fc). The chimeric proteins rhPH20-HSA and rhPH20-Fc performed fairly well as spreading factors in short-term trypan blue intradermal (ID) infusion in comparison with recombinant hyaluronidase (rhPH20). They extended the channel opening from 24 h (rhPH20) to 85–120 h in vivo. The specific activity of rhPH20-Fc was 35,600 U/mg, higher than that of rhPH20-HSA (10,000 U/mg). Co-administration of rhPH20-Fc with two biomacromolecular pharmaceuticals, Stelara (150 KDa) and TNFRII-Fc-IL1ra (TFI, 250 kDa), through an ID route increased the bioavailability from 86% to 93% and from 64% and 97%, respectively, compared with rhPH20. The pharmacokinetic profile of ID administrated larger TFI was significantly improved through cooperation with the long-acting hyaluronidase.

1. Introduction

Subcutaneous (SC) administration for the delivery of biomacromolecular pharmaceuticals provides better safety and convenience than intravenous (IV) administration [1]. However, the bioavailabilities of SC-administered molecules would be lower than the IV route in general, especially for macromolecules [2], when in SC administration, the drugs have to pass through the complex three-dimensional extracellular matrix (ECM) of the dermis and then traverse capillaries or lymphatics in order to reach the general cardiovascular pool [3].

Because the hyaluronan network constitutes the main filler in ECM and serves as a barrier for drug delivery, its breakup could loosen SC space and therefore enhance molecular dispersion [4]. In the past, hyaluronidases extracted from animal tissues were used as chaperone factors [5]. However, undefined impurities and heterogeneous ingredients may cause inflammation. Thus, these hyaluronidases were gradually substituted by recombinant human hyaluronidase rhPH20, which was approved by the FDA in 2005 [6]. As reported, rhPH20 efficiently elevated absolute bioavailabilities of the small molecules ondansetron, morphine and ceftriaxone to 79% [7], 103% [8] and 107% [9], respectively. For biomacromolecular pharmaceuticals, however, the results were not as significant as for the small molecules. Absolute bioavailabilities ranging from 40% to 94% were reported with rhPH20, and required the incorporation of other substances, such as heparin [10–12].

It is possible that the effect of hyaluronidase on the subcutaneous delivery of biomacromolecules is not long enough. Frost [4] reported that the ECM changes induced by rhPH20 were almost reversible within 24 h. This period may be short for macromolecules, whose convection and diffusion are much slower than small molecules. Furthermore, biomacromolecules such as proteins

Abbreviations: SC, subcutaneous; IV, intravenous; ID, intradermal; HA, hyaluronan; ECM, extracellular matrix; BTH, bovine testis hyaluronidase; HSA, human serum albumin; rhPH20, recombinant human PH20; rhPH20-HSA, recombinant human PH20-HSA; rhPH20-Fc, recombinant human PH20-Fc; TFI, TNFRII-Fc-IL1 ra.

* Corresponding authors at: National Key Laboratory of Biochemical Engineering, Institute of Process Engineering, Chinese Academy of Sciences, Beijing, 100190, PR China.
E-mail addresses: mzhui@ipe.ac.cn (M. Hui), zgsu@ipe.ac.cn (Z. Su).
[1] These authors contributed equally to this work.

http://dx.doi.org/10.1016/j.bej.2016.03.013
1369-703X/

are likely to be metabolized in the SC space. Retention in the SC space will lead to longer exposure to catabolic enzymes, while the promotion of intravascular uptake would reduce degradation. The extracellular matrix in the dermis has a complex composition and is made up of an intricate stereochemical structure, which the drugs have to pass through. Therefore, enough open time and space for the ECM "channel" may be helpful to minimize local entrapment and degradation, facilitating the macromolecule diffusion to the vascular compartment successfully. The question is why rhPH20 has so short an action time. Like other proteins, the hyaluronidase can be damaged in the subcutaneous environment through hydrolysis, enzymatic degradation, antigen-antibody reactions, or macrophage ingestion. Although the mechanism is not clear, it would be worthwhile to construct a new hyaluronidase with better durability than the current product against damaging factors, prolonging its role as a channel opener.

The strategy in this paper was to conjugate hyaluronidase with human serum albumin (HSA) or the IgG Fc portion. HSA is the most abundant protein in blood plasma and is widely used as a stabilizing agent for therapeutic proteins in drug formulations. It consists of three conserved homologous structural motifs, each carrying a binding site specific for affinity chromatography [13]. Fusion of heterologous peptides with the IgG Fc portion provides stability for natural proteins [14]. Both HSA and Fc fragments have been used for the conjugation of pharmaceutical drugs and are safe in vivo [15]. Bearing this in mind, we explored whether these reconstruction techniques could improve stability in the dermis and thus exert long-lasting effects. Two pharmaceutical proteins, Stelara (150 kDa) and TFI (250 kDa), were chosen as model molecules to co-administered for pharmacokinetics study. Stelara, also named as ustekinumab, is used to treat patients with relapsing-remitting multiple sclerosis [16]. TFI (TNFR2-Fc-IL-1ra) is a bifunctional ligand with enhanced anti-inflammatory effect [17].

2. Materials and methods

2.1. Materials

Escherichia coli strain Top10 and the cloning plasmid pMD18-T were purchased from Transgene Inc. (Beijing, China) and Takara Bio Inc., (Otsu, Shiga, Japan), respectively. The GC-rich vector pMH and CHO-S cells (routinely cultured in DMEM/F12 or B001 medium) were available in our laboratory. EcoRI and NotI restriction enzymes, T4 DNA ligase and the DNA gel extraction kit were from Takara Bio Inc., (Otsu, Shiga, Japan). All cell culture and transfection reagents were obtained from Invitrogen Corporation (Carlsbad, California, USA) unless specified. The His-tag affinity columns, SP Fast Flow, Q Fast Flow and MabSelect columns were purchased from GE Healthcare (Piscataway, New Jersey, USA). Goat anti-human IgG*HRP, mouse anti-His tag and rabbit anti-human PH20 antibody were obtained from Santa Cruz (Santa Cruz, CA, USA). Bovine testes hyaluronidase (BTH) powder was from Shanghai No. 1 Biochemical Pharmaceutical Co. (Shanghai, China). Nude Balb/c mice (6–8 weeks of age) were purchased from Vital River Laboratory Animal Technology Co., Ltd. (Beijing, China). All animal experiments were in compliance with the Institutional Ethical Committee for animal care guidelines.

2.2. Gene construction and transformation

The plasmid templates for human hyaluronidase PH20, the Fc fragment of human immunoglobulin, human serum albumin, the murine Igκ chain leader sequence and the pMH3 plasmid as expression vector were obtained from AmProtein Inc. (San Gabriel, CA, USA). Primers, shown in Table 1, were designed using Vector NTI and synthesized by Sangon Biotech (Shanghai, China). The pMD18-T plasmid as cloning vector, EcoRI and NotI restriction enzymes, T4 DNA ligase and the DNA gel extraction kit were purchased from Takara Bio Inc. (Dalian, China). The *E. coli* strain Top10 was from Transgene Inc. (Beijing, China).

The scheme for gene construction is delineated in Fig. 1. The gene fragment of PH20 with the EcoR I site synonymously mutated was constructed by overlay PCR using the touch-down procedure with the F1, R1, F2 and R2 primers. Then, the rhPH20 sequence was added with the Igκ signal peptide for protein secretion by overlay PCR, with the F3, R3, F1 and R2 primers. Available rhPH20 with the Igκ signal peptide was then used as the template to overlay with HSA domain I and the Fc fragment of IgG, respectively, for constructing chimeric genes of rhPH20-HSA and rhPH20-Fc. The recombinant genes were all flanked on either side by EcoR I and Not I restriction sites through the PCR primer sequences. The lengths of the gene fragments were verified by DNA electrophoresis.

The chimeric genes were recycled and subcloned into pMD18-T through AT ligation. The mixture was transformed into Top 10 cells to select positive clones. The fidelity of the genes to their original design was verified by PCR, double enzymatic digestion of extracted plasmid with EcoR I and Not I, and DNA sequencing by Sangon (Shanghai, China). The recombinant cloning vectors were digested with EcoR I and Not I, and then the gene fragments were recycled and ligated to the pMH3 expression vector which was similarly digested and recycled. The resulting recombinant plasmids were transformed into CHO host cells along with salmon sperm DNA by electroporation twice at 160 V, 15 ms pulses using an electroporator (Bio-Rad, Richmond, CA, USA).

2.3. Clone screening and recombinant protein expression

For the screening of clones, the transfected cells were maintained in DMEM/F12 medium containing 10% fetal bovine serum (FBS: Invitrogen Life Technologies, Carlsbad, CA, USA) at 37 °C, 5% CO_2. Then, 50 mg/L G418 (Sigma-Aldrich, Shanghai, China) was added two days later. After one week of growth to form visible colonies, pipet tips were used to pick up the cell clumps and the contents were transferred into one well of a 96-well tissue culture plate (Corning, NY, USA). After that, single colonies were enriched through sub-culturing from 96-well plates into 24-well plates in D/F12 medium containing 100 mg/L G418 and subsequently into T25 flasks. The supernatants were collected from either the 96- or the 24-well plates or T25 flasks for the initial assessment of hyaluronidase activity by turbidimetry.

These adherent cultured clones were domesticated and propagated in serum-free medium B001 (AmProtein Inc., San Gabriel, CA, USA) in 40-mL flasks for 2 or 3 weeks. Batch cultures were carried to test the basic expression level for each clone. Clones with the highest expression level were expanded to 1 L spinner flasks, and then transferred to a 5 L bioreactor at an inoculation density of 2.0×10^6 viable cells per mL in B001 medium [18]. We chose single-use bioreactors to carry out cultivation process for their unique features, such as simple operation and low shear force. The parameters were 37 °C, pH 7.2, DO 10–30% and an air overlay of 0–100 cc/min. When the cell density reached $5–6 \times 10^6$, the temperature was reduced to 34 °C, and F001 (AmProtein Inc.) feed medium was added to maintain the residual glucose level at 2 g/L. After approximately 10 days of cultivation, the supernatants were harvested by centrifugation at 5000 rpm for 6 min for purification.

2.4. Purification of recombinant hyaluronidases

Chromatography columns (Q Sepharose FF, Phenyl Sepharose (low sub), SP FF, Blue Sepharose FF, Mabselect and Superdex-200) and the chromatography system (ÄKTA prime) were products of

Table 1
List of primers used in PCR and overlay PCR (restriction sites underlined).

Functions	Corresponding fragments	Primernames	Sequences (5′ to 3′) of primers
Restriction site same sense mutation	PH20-1	F1	*GCTGCTCTGGGTTCCAGGTTCCACTGGTCTGAATTTCAGAGCACCTCCTG*
		R1	*TGAGGTGAAGATAGTCACTTGAGTTCCAGTTTTTCCTTATACACACTC*
	PH20-2	F2	*CAAGGAGTGTGTATAAGGAAAAACTGGAACTCAAGTGACTATCTTCAC*
		R2	*AAGCGGCCGCGTAGAAAATTTGAGGTTCTTCTGTCTCCATG*
Recombination Igκ-PH20	Igκ	F3	*CCCCCAAGCTGGAATTCCACCATGGAGAGAGACACACTCCTGC*
		R3	*ATAACAGGAGGTGCTCTGAAATTCAGACCAGTGGAACCTGGAACCCAGAG*
	PH20	F1	*GCTGCTCTGGGTTCCAGGTTCCACTGGTCTGAATTTCAGAGCACCTCCTG*
		R2	*AAGCGGCCGCGTAGAAAATTTGAGGTTCTTCTGTCTCCATG*
Recombination Igκ-PH20-HSA	Igκ-PH20	F3	*CCCCCAAGCTGGAATTCCACCATGGAGAGAGACACACTCCTGC*
		R4	*AGCAACCTCACTCTTGTGTGCATCGTAGAAAATTTGAGGTTCTTCTGTCTCC*
	HSA	F4	*TGGAGACAGAAGAACCTCAAATTTTCTACGATGCACACAAGAGTGAGGTTG*
		R5	*AAGCGGCCGCTTACTATCTCTGTTTGGCAGACGAAGC*
Recombination Igκ-PH20-Fc	Igκ-PH20	F3	*CCCCCAAGCTGGAATTCCACCATGGAGAGAGACACACTCCTGC*
		R6	*CGGTGGGCACTCGACGTAGAAAATTTGAGGTTCTTCTGTCTCC*
	Fc	F5	*AGACAGAAGAACCTCAAATTTTCTACGTCGAGTGCCCACCGTG*
		R7	*AAGCGGCCGCTTACTATTTACCCGGAGACAGGGAGAG*

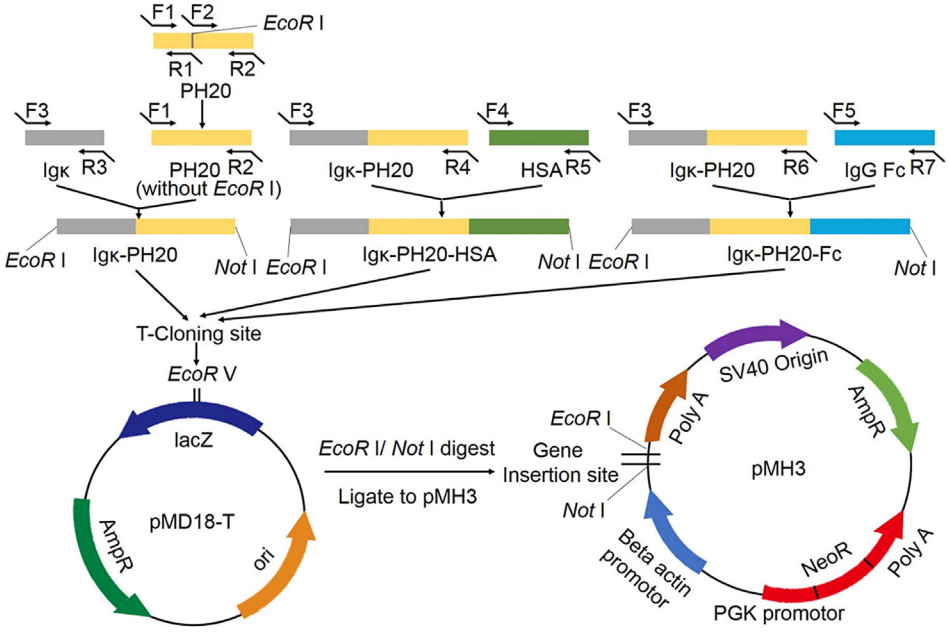

Fig. 1. Sketch of construction of recombinant genes, cloning vectors and expression vectors.

GE Healthcare Bio-Sciences (Uppsala, Sweden). The CHT ceramic hydroxyapatite column was from Bio-Rad (Richmond, CA, USA).

The collected supernatant of 3–3.5 L was filtered through a Supor membrane disc filter of 293 mm in diameter (Pall Life Sciences, Michigan, USA) with sequential membranes which had pore sizes of 0.8 μm, 0.45 μm and 0.22 μm, respectively. The supernatant was submitted to tangential flow diafiltration with a Pellicon cassette system (NMWCO of 30 kDa, Millipore, Massachusetts, USA). The filtrate volume was reduced to 600–700 mL at this step. The buffer was mainly replaced to 20 mM Tris buffer at pH 7.4 with 50 mM NaCl for rhPH20 and rhPH20-HSA, and the same buffer with 100 mM NaCl for rhPH20-Fc.

The preparation of rhPH20 was initiated using two tandem Q Sepharose FF columns (20 cm × 2.6 cm I.D.) previously equilibrated with 20 mM Tris buffer at pH 7.4 with 50 mM NaCl. The weakly bound fractions were washed out with the same buffer at pH 7.0. The absorbed proteins were eluted at 380 mM NaCl, pH 7.0. The eluent was then diluted with 2 M $(NH_4)_2SO_4$ and 500 mM $CaCl_2$ to a final concentration of 500 mM $(NH_4)_2SO_4$ and 0.1 mM $CaCl_2$ and then loaded onto a Phenyl Sepharose (low sub) column (20 cm × 2.6 cm I.D.). The flow-through fraction was collected and diluted with degassed water to a conductivity of 7.5 mS/cm and the pH was adjusted with HAc to 5.4. Afterwards, the solution was loaded onto an SP fast flow column (20 cm × 2.6 cm I.D.) pre-equilibrated with 20 mM HAc/NaAc buffer at pH 5.4 with 50 mM NaCl, and then eluted at 130 mM NaCl in the same buffer. The eluted fraction was adjusted to pH 7.0 and loaded onto a CHT ceramic hydroxyapatite column (12 cm × 2.6 cm I.D., Bio-Rad) pre-equilibrated with 10 mM PB and 1 mM $CaCl_2$ at pH 7.0. The bound proteins were eluted with 80 mM PB and 0.1 mM $CaCl_2$ at pH 7.0.

For rhPH20-HSA purification, the protein solution was loaded onto a Q Sepharose FF column (20 cm × 2.6 cm I.D.) previously equilibrated with 20 mM Tris and 50 mM NaCl at pH 7.4. The weakly bound fractions were washed out with 20 mM Tris and 120 mM NaCl at pH 7.0. The bound proteins were eluted at 450 mM NaCl at pH 7.0. The eluent was diluted 2.25 times with degassed water and then loaded onto a Blue Sepharose Fast Flow column (18 cm × 2.6 cm I.D.) pre-equilibrated with 20 mM Tris and 200 mM NaCl at pH 7.0. The column was washed with 200 mM KCl in pH 7.0 Tris buffer, and the fractions were eluted with 600 mM KCl in pH 7.0 Tris buffer. The active fractions were then diluted with 2 M $(NH_4)_2SO_4$ and 500 mM $CaCl_2$ to a final concentration of 500 mM $(NH_4)_2SO_4$ and 0.1 mM $CaCl_2$ and then loaded onto a Phenyl Sepharose (low sub) column (20 cm × 2.6 cm I.D.). The

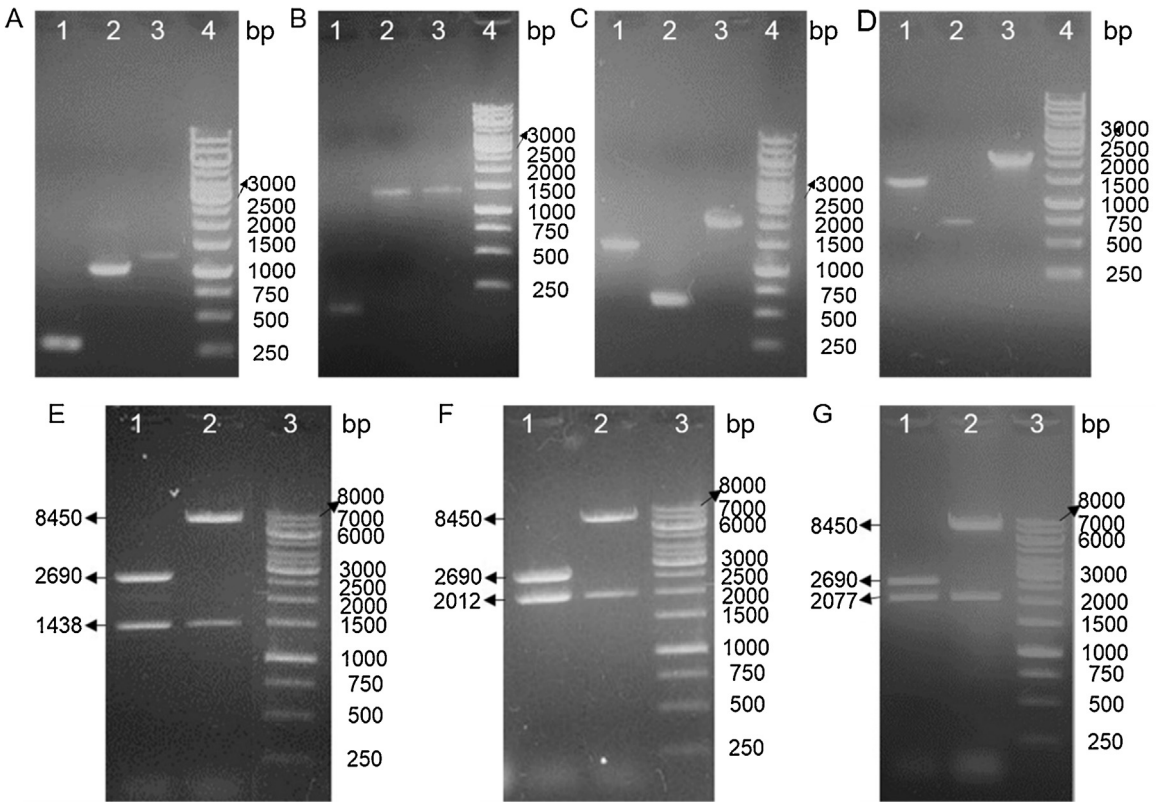

Fig. 2. Construction of fused genes and recombinant vectors. (A)–C): Overlay PCR for (A) PH20 without EcoR I (lane 1: PH20-1, lane 2: PH20-2, lane 3: PH20 without EcoR I); (B) Igκ-PH20 (lane 1: Igκ, lane 2: PH20 without EcoR I, lane 3: Igκ-PH20); (C) Igκ-PH20-HSA (lane 1: Igκ-PH20, lane 2: HSA, lane 3: Igκ-PH20-HSA); (D) Igκ-PH20-Fc (lane 1: Igκ-PH20, lane 2: Fc, lane 3: Igκ-PH20-Fc). (E)–(G): Cloning vectors and expression vectors for (E) rhPH20 (lane 1: pMD18-T-Igκ-PH20/EcoR I+ Not I, lane 2: lane 1: pMH3-T-Igκ-PH20/EcoR I+ Not I); (F) rhPH20-HSA (lane 1: pMD18-T-Igκ-PH20-HSA/EcoR I+ Not I, lane 2: lane 1: pMH3-T-Igκ-PH20-HSA/EcoR I+ Not I); (G) rhPH20-Fc (lane 1: pMD18-T-Igκ-PH20-Fc/EcoR I+ Not I, lane 2: lane 1: pMH3-T-Igκ-PH20-Fc/EcoR I+ Not I).

columns were washed with 0.25 M $(NH_4)_2SO_4$ in Tris buffer, and the fractions were eluted by the same buffer without $(NH_4)_2SO_4$.

To purify rhPH20-Fc, the solution was loaded onto a Mabselect column (17 cm × 5.0 cm I.D.) in 20 Tris buffer at pH 7.4 with 100 mM NaCl and eluted with a buffer containing 50 mM Arg, 100 mM Gly (pH 3.5) and 0.01% Tween-80. The active fractions were pooled and loaded onto Q SFF columns (12 cm × 2.6 cm I.D.) pre-equilibrated with 20 mM His and 50 mM NaCl at pH 6.0, and eluted with 20 mM His buffer containing 150 mM NaCl at pH 5.5. The eluent was loaded onto a Superdex-200 column and eluted with 100 mM phosphate buffer at pH 7.0.

The purification procedures were controlled by ÄKTA prime, and the signals at UV–280 nm and the conductivity of the effluent were monitored. The protein concentration was measured with a Protein Assay Kit (Bio-Rad, Richmond, CA, USA) with BSA used as the standard [19]. The purity of the purified protein was determined by HPLC. It was also subjected to SDS-PAGE and identified by western blotting.

2.5. SDS-PAGE and western blotting

SDS-PAGE was performed as described by Laemmli [20]. Protein samples were resolved in 8% (w/v) polyacrylamide gel. After electrophoresis, the proteins were visualized by staining with Coomassie Brilliant Blue R-250. For western blot analysis, the proteins resolved in the gel were transferred to polyvinylidene difluoride (PVDF) membranes (Millipore, Massachusetts, USA). The membrane was blocked with 5% BSA in TBST buffer (20 mM Tris-HCl, pH 8.0, 150 mM NaCl, 0.15% Tween-20) at room temperature for 1 h, and then incubated with rabbit anti-human rhPH20 (Santa Cruz Biotechnology, Inc., Santa Cruz, CA, USA) (at a dilution ratio of 1:1000 in TBST containing 1% BSA) at room temperature overnight. The membrane was washed three times with TBST buffer and then incubated with goat anti-rabbit IgG*HRP antibody (ThermoFisher Scientific, San Jose, CA, USA) (at 1:5000 dilution in TBST containing 1% BSA) at 30 °C for 2 h. The membrane was then washed three times with TBST followed by detection using HRP.

2.6. HPLC profile

The final purified protein was assayed using a Waters Breeze HPLC system (Waters Corporation, Milford, MA, USA) on a 200 mm × 7.8 mm Protein-Pak 125 column. The column was equilibrated and eluted with sodium phosphate (pH 7.4) at a flow rate of 0.5 mL/min. Proteins were detected at 280 nm. Purity was determined according to the percentage of the main peak area [21].

2.7. Microtiter-based assay of hyaluronidase activity

Hyaluronidase activity was conducted viscosimetrically according to published recommendations [22]. Briefly, bovine testes hyaluronidase (BTH: Shanghai No. 1 Biochemical Pharmaceutical Co., Shanghai, China) powder with an activity of 1500 U/ampoule was dissolved in sterile water and diluted with 1.3 mg/mL hydrolyzed gelatin to obtain a series of concentrations of 0, 0.3, 0.6, 0.9, 1.2, and 1.5 U/mL as standards. Twenty-five microliters of HA (0.25 mg/mL) in an acetate/kalium aceticum buffer was mixed with 25 μL of enzyme and digested at 37 °C for half an hour. Subsequently, two hundred microliters of acidified bovine serum was added. This mixture was finally incubated at room temperature for 1 h. High molecular HA formed a complex with the acidified serum with a maximum absorption at 650 nm. Because hyaluronidase

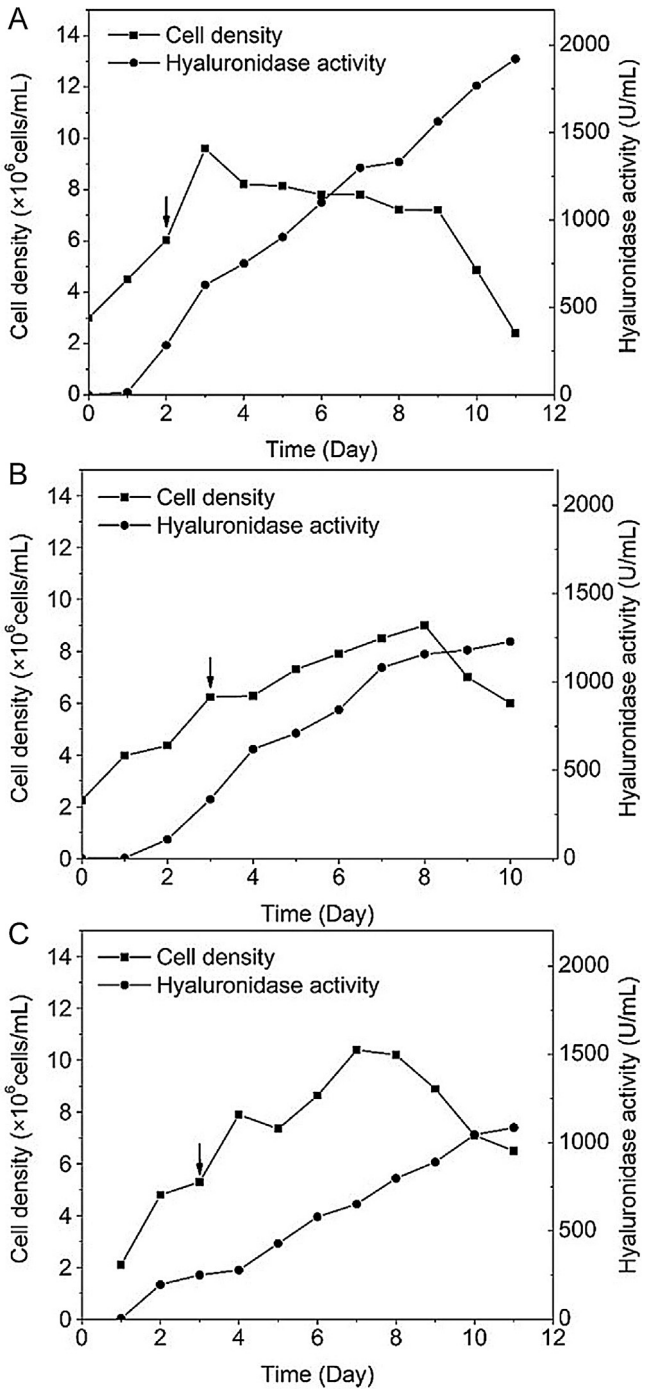

Fig. 3. Expression of hyaluronidase under batch-fed cultivation conducted in disposable bioreactors of 5 L (working volume). (A) rhPH20; (B) rhPH20-HSA; (C) rhPH20-Fc.

activity leads to a decrease in high molecular HA, complex formation and absorption at 650 nm is reduced depending on the incubation time. Hyaluronidase activity was calculated on the basis of the decrease in absorption at 650 nm.

2.8. Interstitial dispersion experiments and reconstruction of dermis

For interstitial dispersion assays, the Balb/c nude mice (Weitonglihua, Beijing, China) were anesthetized by ethyl ether. Subsequently, the mice were injected on the back with trypan blue and test article (0.5 U of rhPH20, rhPH20-HSA, or rhPH20-Fc, or bovine hyaluronidase as positive control) as adjuvant or preparation as carrier control in a 1-mL syringe with a 27 gauge needle in a final volume of 50 μL. Afterwards, dye areas were measured at the specific time points using microcalipers in two dimensions. The areas were calculated using the formula = $((D1 \times D2) \times \pi/4)$ (where D1 and D2 are the diameters of the dye front). For dermal barrier reconstitution experiments, hyaluronidase reference standard, rhPH20, rhPH20-HSA or rhPH20-Fc was injected and marked with a pen at the exact site [4]. Trypan blue was injected in dermal at the marked site after 0.5, 1, 24, 48, 72, 96 and 120 h. Dye areas were measured as above.

2.9. Pharmacokinetics and bioavailability of macromolecules co-injected with hyaluronidase

Stelara (15 mg/kg) or TFI (5 mg/kg) in 100 μL saline was administered in four groups of ICR mice (five per group) anesthetized with ethyl ether via four routes: (1) intravenous injection (group 1); (2) intradermal injection in the dermis received 50 μL carrier vehicle (PBS) (group 2); (3) intradermal injection in the dermis treated with 100 units rhPH20 (group 3); (4) intradermal injection with 100 units rhPH20-Fc (group 4). The treatments were given just before Stelara/TFI injection. Then, 100 μL of blood was collected via tail bleed at 1 h, 2 h, 4 h, 6 h, 24 h, 48 h and 96 h. Serum concentrations of intact TFI were measured by ELISA assay with TNFR II and IL-1ra antibody, respectively. Serum concentrations of intact Stelara were measured by ELISA assay with Fc and F(ab′)2 antibody, respectively. Pharmacokinetic parameters were established using the linear trapezoidal method with integration from T0 to infinity based upon the elimination rate constants established from the intravenous doses.

2.10. Statistical analysis

All statistical analyses were performed using GraphPad Prism 5 software (GraphPad Software, San Diego, CA, USA).

3. Results and discussion

3.1. Construction of recombinant cell lines expressing hyaluronidase

As shown in Fig. 2A, the newly constructed gene fragment of PH20 without EcoR I was verified by DNA electrophoresis. Because EcoR I ligates with the vector backbone afterward cloning, it is necessary to omit the EcoR I site within the original PH20 sequence through synonymous mutation. Then, as shown in Fig. 2B, Igκ signal peptide was successfully added to the N-terminal of PH20. As a consequence, the fusion proteins would be secreted into the supernatant during cultivation [23]. Fig. 2C and D show overlaid gene fragments encoding Igκ-PH20-HSA and Igκ-PH20-Fc, respectively, and verification by DNA electrophoresis.

As shown in Fig. 2E–G, three fused gene fragments of Igκ-rhPH20, Igκ-rhPH20-HSA and Igκ-rhPH20-Fc were successfully ligated to the cloning vector pMD18-T and expression vector pMH3, respectively. The sizes of the gene fragments resulting from EcoR I and Not I double digestion were 1438 bp, 2012 bp and 2077 bp, and PCR verifications were as expected. Furthermore, based on the sequencing results, no unexpected mutation or deletion was observed during the cloning process, confirming the fidelity of the sequence with the original design.

PH20 is a relatively complex molecule with six *N*-glycosylation sites and five disulfide bonds. Both the domain I of HSA used here and the Fc fragment of IgG2 have glycosylation sites and intrachain disulfide bonds, as well as interchain disulfide bonds for the Fc fragment. Therefore, choosing a proper expression system is critical for

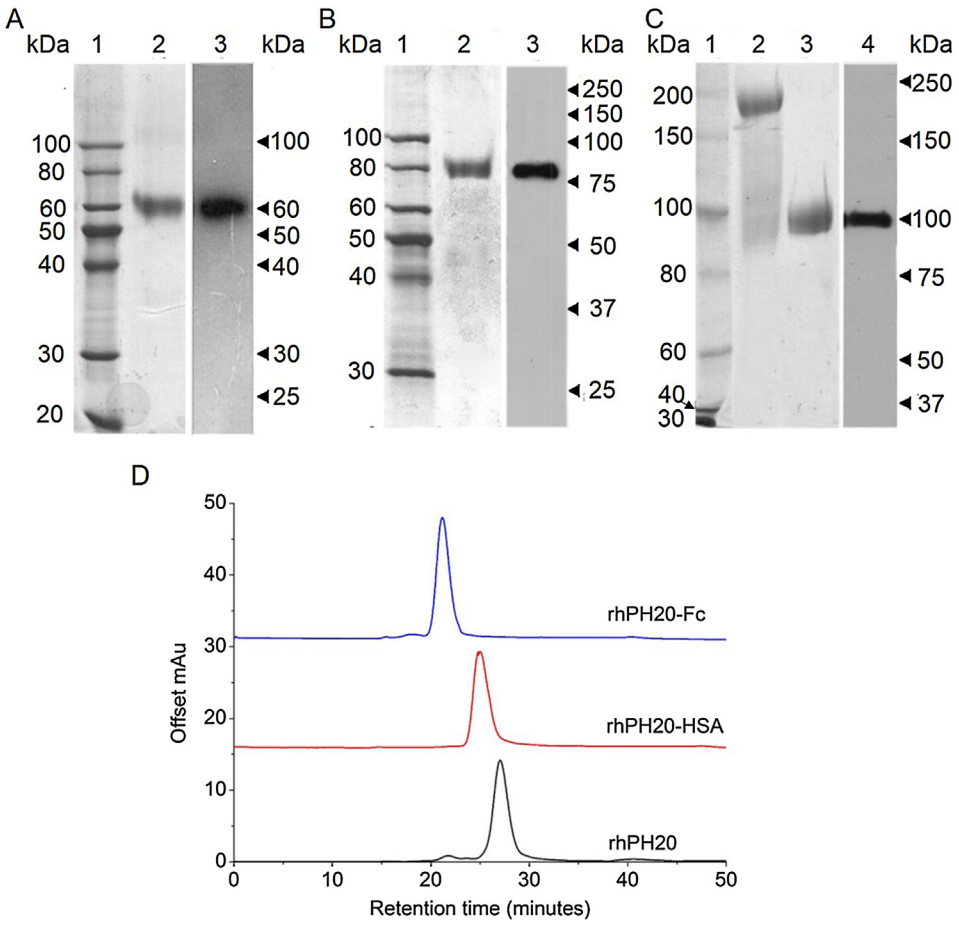

Fig. 4. SDS PAGE, Western blot and HPLC profile. (A) rhPH20 (Lane 1: Marker in SDS-PAGE analysis; lane 2: non-reducing form of rhPH20 in SDS-PAGE analysis; lane 3: Western blot analysis). (B) rhPH20-HSA (Lane 1: Marker in SDS-PAGE analysis; lane 2: non-reducing form of rhPH20-HSA in SDS-PAGE analysis; lane 3: Western blot analysis). (C) rhPH20-Fc (Lane 1: Marker in SDS-PAGE analysis; lane 2: non-reducing form of rhPH20-Fc in SDS-PAGE analysis; lane 3: reducing form of rhPH20-Fc in SDS-PAGE analysis; lane 4: Western blot analysis). (D) HPLC profile of purified recombinant proteins. From top to bottom the curves represent rhPH20-Fc, rhPH20-HSA and rhPH20, respectively.

successfully characterizing posttranslational modifications and the correct features of the chimeric proteins. Chinese hamster ovary (CHO) cells meet the requirements and are an attractive choice for the production of complex proteins [24]. However, a low efficiency of production is a problem for CHO. To remove this issue, both choosing specific expression vectors and the introduction of salmon sperm DNA during transfection are of assistance.

After gene transfection, two-cycle clone selection and adaption to suspension culture, three stable and high-level expression clones for each protein were chosen from thousands of clones and were used for subsequent expression. The basic expression levels of batch culture in 40-mL flasks for each of the selected clones were 1490, 596, and 737 U/mL for rhPH20, rhPH20-HSA and rhPH20-Fc, respectively.

3.2. Cultivation for recombinant hyaluronidase

As shown in Fig. 3, the cultivation processes are divided into the growth stage and the production stage. In the cell growth stage, a high specific growth rate is expected to achieve a high cell density. On the other hand, in the production stage, after lowering the temperature to 34 °C, a high specific production rate is stressed for the expression and secretion of the desired protein. During the cultivation process, cell concentrations increased to $5–6 \times 10^6$ at the second or third day, reached a maximum of $9–10 \times 10^6$ cells/mL from the third to seventh day, and then decreased with time. The accumulation of hyaluronidase increased gradually at the initial stage, and although the cell concentration decreased, expression continued to increase. The fed-batch culture was carried out for 10–11 days, at which the cell viability was below 80%. These processes resulted in a final production of 1900, 1085, and 1228 U/mL for rhPH20, rhPH20-HSA and rhPH20-Fc, respectively.

3.3. Purification and identification of recombinant hyaluronidase

The purified recombinant hyaluronidases were subjected to SDS-PAGE and western blotting to determine the apparent molecular weights and antigenic specificity, as shown in Fig. 4. The purified recombinant hyaluronidases rhPH20, rhPH20-HSA and rhPH20-Fc were 61 kDa (Fig. 4A), 79 kDa (Fig. 4B), 190 kDa (non-reducing form) and 95 kDa (reducing form) (Fig. 4C), respectively. The molecular weight of rhPH20 was consistent with the results in the literature for a soluble form of neutral-active human hyaluronidase (PH20) lacking the GPI membrane attachment motif [4]. The size of rhPH20-HSA was equivalent to the combination of rhPH20 and domain I of HSA. rhPH20-Fc was an antibody-like dimer structure in non-reducing conditions, which was linked by interchain disulfide bonds and the variable region was replaced by PH20.

To confirm the antigenic activity of the recombinant hyaluronidases, the protein resolved by SDS-PAGE was subjected to western blot analysis using anti-human rhPH20 monoclonal antibody. As shown in Fig. 4, a single band was detected by the antibody for each protein, indicating their antigenic activity.

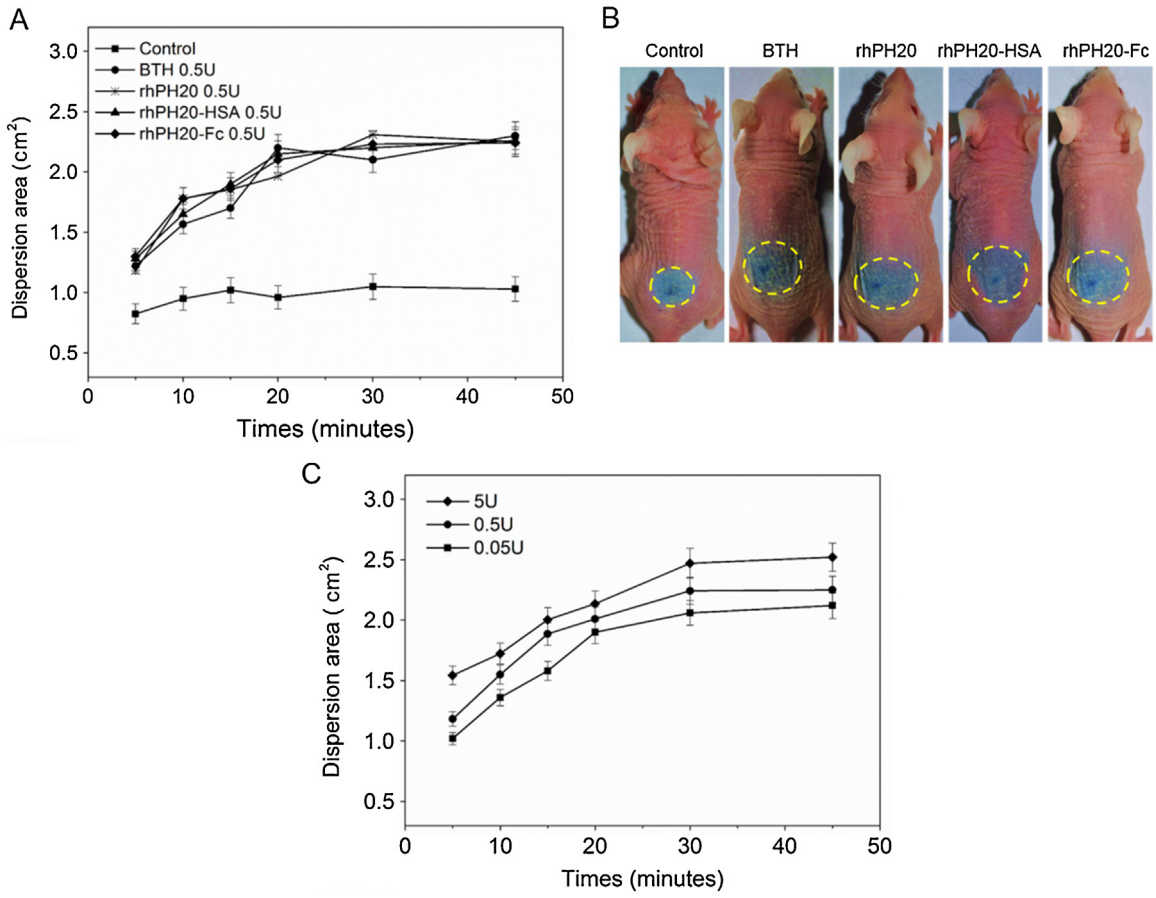

Fig. 5. Diffusion properties of trypan blue with hyaluronidase co-administration in dermis. (A) rhPH20, rhPH20-Fc, rhPH20-HSA, bovine hyaluronidase (0.5 U), or carrier control was co-injected with trypan blue in mice. (B) Trypan blue diffusion 45 min after combined injection with carrier, rhPH20, bovine hyaluronidase, rhPH20-Fc or rhPH20-HSA (from left to right). (C) rHuPH20-Fc (5.0, 0.5, 0.05 U) was co-injected with trypan blue in mice. (For interpretation of the references to colour in this figure legend, the reader is referred to the web version of this article.)

From the HPLC profile shown in Fig. 5, the purified recombinant hyaluronidases were eluted as single peaks at 21.17, 25.02 and 27.03 min from a Protein-Pak 125 column. The purity was more than 95%. The purified rhPH20, rhPH20-HSA and rhPH20-Fc exhibited a specific activity of 100,000, 10,000 and 35,600 U/mg protein by the micro turbidity assay. In addition, the endotoxin activities for each purified protein were less than 0.1 U/mg, suggesting that highly purified recombinant hyaluronidase preparations could be considered as a potential therapeutic agent for pharmacodynamics studies.

3.4. Spreading effects of recombinant human hyaluronidases

Hyaluronan confers hygroscopicity and swelling capacity to the ECM, while molecules administered through SC are sequestered within it. Spreading to the vessels is a prerequisite for drugs for being absorbed [25]. In this manuscript, we used intradermal injection of mice as a simple animal model for human subcutaneous injection. As the hypodermis of mouse is very loose, drugs may move quickly without striking barriers, so it is not predictive for clinical SC injection outcomes. However, the epidermis of mice is closer to the thickness of human dermis than mouse hypodermis, and could be more predictive for drug diffusion and absorption in clinical use. The potency of different hyaluronidases as spreading factors can be determined by their abilities to increase the area of locally injected tracer dyes following intradermal co-administration [26]. Trypan blue dispersion experiments for 45 min represent the diffusion-promotion in a short period. As shown in Fig. 5, when co-injected with 0.5 U rhPH20-HSA and rhPH20-Fc, trypan blue exhibited comparable diffusion profiles with the 0.5 U bovine hyaluronidase and rhPH20 treatments (Fig. 5A), and all of them reached similar dye areas of approximately 2.2 cm^2 at 45 min (Fig. 5B). Because the specific activities of rhPH20-HSA and rhPH20-Fc were inferior to the original rhPH20, one-tenth and one-third, respectively, a higher dosage of rhPH20-HSA and rhPH20-Fc is needed to achieve a biological effect analogous to the original rhPH20 in a short time frame.

The dose-response relationships were explored for the newly constructed hyaluronidase, with rhPH20-Fc as a model. As shown in Fig. 5C, from the first detection time point, trypan blue diffused to a larger area in the high rhPH20-Fc dose, which indicated that the facilitated diffusion effect of rhPH20-Fc occurred in a dose-dependent fashion, in agreement with rhPH20 [4].

In SC administration, molecules must diffuse and be absorbed to exert influence. The complex three-dimensional structure of ECM physically retards molecular dispersion [27]. The degradation of hyaluronan and the openness of the ECM channel influence diffusion and absorption. Therefore, the process of ECM recovery after hyaluronidase treatment was of key importance for SC-administered molecules. As shown in Fig. 6, each point stood as the termination of trypan blue dispersion experiments at 45 min. The pink shadow represents the primary trypan blue diffusion level and almost complete recovery. When the dermis was treated with rhPH20 after 24 h, it was repaired and was resistant to trypan blue again. The groups treated with rhPH20-Fc were not reconstructed until 85 h, and the groups treated with rhPH20-HSA needed 120 h.

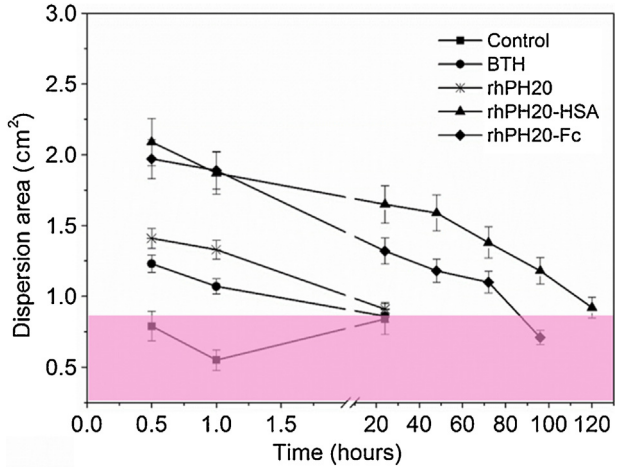

Fig. 6. Reconstruction of dermis after treatment with different hyaluronidases.

The changes in tissue structure due to different hyaluronidases were all reversible. Comparably, the accessible pathway created by rhPH20-HSA and rhPH20-Fc lasted much longer than bovine hyaluronidase and rhPH20.

The recombination of human hyaluronidase in this study successfully extended its functioning time in dermis. Subcutaneous architecture is a key factor for penetration and metabolism of administered therapeutics, so it is reasonable that its change would exert an influence on pharmacokinetics and bioavailabilities [28]. Short-time destruction of the ECM provided a traverse channel for small molecules. On the other hand, the diffusion and convection of large molecules occurred in a slower pattern and a long channel-opening time was needed for thorough diffusion. Enough open time and space for the ECM channel would be favorable for macromolecules to fully diffuse to the vascular compartment. The original rhPH20 and long-acting recombinant hyaluronidase meet the specific demands of small molecules and macromolecules.

3.5. *Pharmacokinetic profiles for co-administration with recombinant long-acting hyaluronidase rhPH20-Fc*

Modifying ECM architecture is an effective method to alter the pharmacokinetic profile of SC therapeutics through increasing their exposure to the capillary beds and lymphatics [29]. Considering that the specific activity of rhPH20-Fc was better than rhPH20-HSA, it was chosen for co-injection with the two therapeutics, and the pharmacokinetics were investigated.

As shown in Fig. 7, the effects of rhPH20 and rhPH20-Fc on the pharmacokinetics and bioavailability of a 149 kDa Stelara and 250 kDa TFI were assessed. As expected, the pharmacokinetic (PK) profiles following IV and SC administration differed greatly. Generally, intravenous IgG administration resulted in early high peak concentrations, followed by a rapid fall over the next several days, which was associated with the passage of proteins from the vasculature to the lymph and extracellular fluid compartments [29]. When administered via the SC route (here the mouse ID was used as a suitable surrogate for human SC), the proteins distributed initially in the local subcutaneous tissue, followed by slow diffusion into the vascular and extravascular fluid space [27]. Because peak serum levels of SC are lower, the adverse effects associated with very high peaks experienced after large IV boluses would be much less common.

As shown in Table 2, rhPH20 and rhPH20-Fc improved the AUC of Stelara from 6.5 k to 9.6 k and 10.4 k μg H/mL, with an absolute bioavailability increase from 58% to 86% and 93%. There was a 7% increase between rhPH20 and rhPH20-Fc. The T_{max} shifted from 24 h to 6 h and C_{max} was higher for the two hyaluronidase-facilitated groups. For TFI, there was significant increase in AUC. rhPH20 and rhPH20-Fc improved the AUC from 1079.6 to 1356.6 and 2053.7 μg H/mL, with an absolute bioavailability from 51% to 64% and 97%, very close to that of IV. SC administration combined with long-acting rhPH20-Fc achieved a bioavailability similar to IV. Also, instead of the early high peak concentrations resulted from intravenous administration, when administered via the co-administration SC route, the proteins distributed initially in the local subcutaneous tissue, followed by slow diffusion into the vascular and extravascular fluid space.

There are factors affecting the bioavailability data that we must take into account. For example, 0.1 mL blood samples were collected for each time. Within 24 h, another 0.5 mL blood was collected; i.e., ca. 25% of the blood volume in a 20 g mouse. This high-volume blood sampling contributed in a relevant manner to the clearance of the administered drug, particularly after IV dosing. Hence, there is the possibility of overestimation of SC bioavailability. IV administration would be more affected by pronounced sampling compared to SC administration because during the phase of intense sampling (1–24 h), drug levels after IV dosing are markedly higher than after SC dosing. However, the comparable relationship between different administration routes would not be affected greatly.

The improvement of pharmacokinetics can be ascribed to the facilitated convection of these macromolecules. In particular, rhPH20-Fc performed better than rhPH20 on facilitating the permeation of the large molecule TFI and elevating its bioavail-

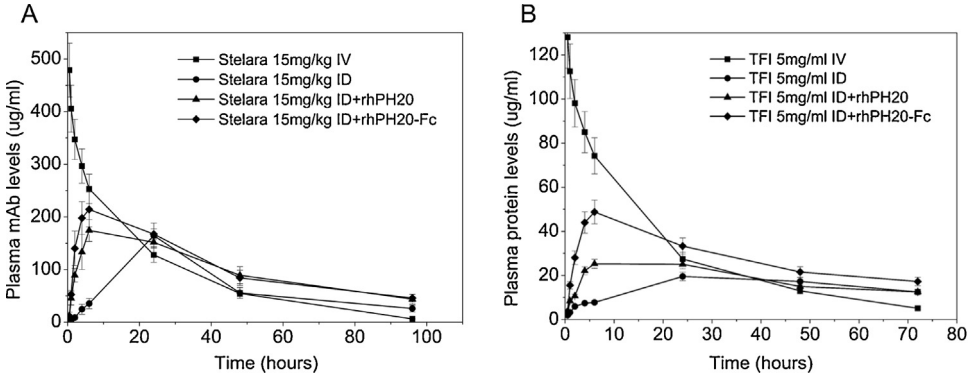

Fig. 7. Pharmacokinetic profiles of Stelara (A) and TFI (B) injected subcutaneously with hyaluronidase in comparison to intravenous (IV) and intradermal (ID).

Table 2
Summary of pharmacokinetic parameters for molecules co-injected with hyaluronidase subcutaneously or intravenously. IV, intravenous; ID, intradermal.

Groups	AUC (μg h/mL)	F (%)	T_{max} (h)	C_{max} (μg/mL)
Stelara 15 mg/kg IV	11209.3 ± 1105.2	100 ± 9.9	0.5	478.9 ± 48.4
Stelara 15 mg/kg ID	6493.4 ± 570.3	57.9 ± 5.1	24	164.6 ± 23.8
Stelara 15 mg/kg ID + rhPH20	9624.4 ± 740.4	85.9 ± 6.6	6	174.3 ± 20.9
Stelara 15 mg/kg ID + rhPH20-Fc	10432.5 ± 745.0	93.1 ± 6.6	6	214.1 ± 33.0
TFI 5 mg/kg IV	2125.2 ± 193.6	100 ± 9.1	0.5	128.1 ± 13.8
TFI 5 mg/kg ID	1079.6 ± 92.3	50.8 ± 4.3	24	19.6 ± 1.8
TFI 5 mg/kg ID + rhPH20	1356.6 ± 113.4	63.8 ± 5.3	6	25.3 ± 2.0
TFI 5 mg/kg ID + rhPH20-Fc	2053.7 ± 162.5	96.6 ± 7.6	6	48.8 ± 5.4

ability. RhPH20-Fc as a promoter drug presented higher stability than rhPH20 in the dermis. In addition because the channels of ECM opened up by long-acting hyaluronidase rhPH20-Fc in this study were sustained for a long time, drugs may permeate much thoroughly and therefore the pharmacokinetics were improved.

Co-administration with hyaluronidase rendered a more gradual PK profile with slow and sustained drug release. This pattern is particularly suitable for some macromolecular proteins to remain at low doses in the circulation. The spreading effect of rhPH20-Fc is quite attractive in the SC administration of macromolecular biotherapeutics, as an effective, safe and easy-to-handle SC drug delivery system. It's worth mentioning that PH20 has been proven safe in clinical trials and on market for several years. Both of HSA and IgG Fc conjugations have been used for intravenous administration of proteins, and there are no adverse effects found so far. Yet there should be more to do with the new hyaluronidases, and a systematic investigation on toxicity and pharmacology is required for the molecules to become clinically acceptable.

4. Conclusions

The newly designed chimeric hyaluronidases, rhPH20-Fc and rhPH20-HSA, are better chaperones than previous rhPH20 for subcutaneous administration of biopharmaceuticals because of their ability to extend the opening time of channels in the extracellular matrix, thus facilitating large molecules to penetrate though. This has been demonstrated by the dermis reconstruction testing where rhPH20 only extended the opening time of ECM channels for 24 h, while rhPH20-HSA and rhPH20-Fc could reach 85–120 h. The specific activity of rhPH20-Fc is higher than that of rhPH20-HSA. The improvement by rhPH20-Fc as a chaperone for Stelara (150 kDa) was obvious but not significant over rhPH20. However, for TFI with molecular weight 250 kDa, PH20-Fc performed much better than rhPH20. Compared with injection alone, co-administration of the large biopharmaceuticals with rhPH20-Fc improved T_{max} as well as C_{max}. In addition, the pharmaceutical profiles were optimized in a gradual change mode. This study is a step forward in development of subcutaneous administration for the delivery of biomacromolecular pharmaceuticals.

Acknowledgements

This research was supported by the National High Technology Research and Development Program of China (No. 2012AA021202) and the National Key Basic Research Program of China (No. 2013CB733600).

References

[1] K.L. Stoner, H. Harder, L.J. Fallowfield, V.A. Jenkins, Intravenous versus subcutaneous drug administration. Which do patients prefer? A systematic review, Patient-Patient-Centered Outcomes Res. (2014) 1–9.
[2] W.F. Richter, B. Jacobsen, Subcutaneous absorption of biotherapeutics: knowns and unknowns, Drug Metab. Dispos. 42 (2014) 1881–1889.
[3] M. Grant, A. Leone-Bay, Peptide therapeutics: it's all in the delivery, Ther. Deliv. 3 (2012) 981–996.
[4] L.H. Bookbinder, A. Hofer, M.F. Haller, M.L. Zepeda, G.A. Keller, J.E. Lim, T.S. Edgington, H.M. Shepard, J.S. Patton, G.I. Frost, A recombinant human enzyme for enhanced interstitial transport of therapeutics, J. Control. Release. 114 (2006) 230–241.
[5] E. Chain, E. Duthie, Identity of hyaluronidase and spreading factor, Br. J. Exp. Pathol. 21 (1940) 324.
[6] G.I. Frost, Recombinant human hyaluronidase (rHuPH20): an enabling platform for subcutaneous drug and fluid administration, Expert Opin. Drug. Deliv. 4 (2007) 427–440.
[7] S.S. Dychter, R. Harrigan, J.D. Bahn, M.A. Printz, B.J. Sugarman, E. DeNoia, D.B. Haughey, D. Fellows, D.C. Maneval, Tolerability and pharmacokinetic properties of ondansetron administered subcutaneously with recombinant human hyaluronidase in minipigs and healthy volunteers, Clin. Ther. 36 (2014) 211–224.
[8] J.R. Thomas, M.S. Wallace, R.C. Yocum, D.E. Vaughn, M.F. Haller, J. Flament, The INFUSE-morphine study: use of recombinant human hyaluronidase (rHuPH20) to enhance the absorption of subcutaneously administered morphine in patients with advanced illness, J. Pain. Symptom Manage. 38 (2009) 663–672.
[9] G. Harb, F. Lebel, J. Battikha, J.W. Thackara, Safety and pharmacokinetics of subcutaneous ceftriaxone administered with or without recombinant human hyaluronidase (rHuPH20) versus intravenous ceftriaxone administration in adult volunteers, Curr. Med. Res. Opin. 26 (2010) 279–288.
[10] R.L. Wasserman, Progress in gammaglobulin therapy for immunodeficiency: from subcutaneous to intravenous infusions and back again, J. Clin. Immunol. 32 (2012) 1153–1164.
[11] B. Bittner, W.F. Richter, F. Hourcade-Potelleret, C. McIntyre, F. Herting, M.L. Zepeda, J. Schmidt, Development of a subcutaneous formulation for trastuzumab—nonclinical and clinical bridging approach to the approved intravenous dosing regimen, Arzneimittelforschung 62 (2012) 401–409.
[12] S. Zollner, H. Metzner, Combined use of a sulfated glycosaminoglycan and a hyaluronidase for improving the bioavailability of factor VIII, US Patent 20,150,023,946, 2015.
[13] M. Dockal, D.C. Carter, F. Ruker, The three recombinant domains of human serum albumin structural characterization and ligand binding properties, J. Biol. Chem. 274 (1999) 29303–29310.
[14] H. Watier, Variability factors in the clinical response to recombinant antibodies and IgG Fc-containing fusion proteins, Expert Opin. Biol. Ther. 5 (2005) S29–S36.
[15] L. Diao, B. Meibohm, Pharmacokinetics and pharmacokinetic-pharmacodynamic correlations of therapeutic peptides, Clin. Pharmacokinet. 52 (2013) 855–868.
[16] B.M. Segal, C.S. Constantinescu, A. Raychaudhuri, L. Kim, R. Fidelus-Gort, L.H. Kasper, U.M. Investigators, Repeated subcutaneous injections of IL12/23 p40 neutralising antibody, ustekinumab, in patients with relapsing-remitting multiple sclerosis: a phase II double-blind, placebo-controlled, randomised, dose-ranging study, Lancet Neurol. 7 (2008) 796–804.
[17] B. Xie, S. Liu, S.Y. Wu, A. Chang, W.Y. Jin, Z.X. Guo, S.D. Ye, M.Z. Hui, A novel bifunctional protein TNFR2-Fc-iL-1ra (TFI): expression, purification and its neutralization activity of inflammatory factors, Mol. Biotechnol. 54 (2013) 141–147.
[18] R. Eibl, S. Kaiser, R. Lombriser, D. Eibl, Disposable bioreactors: the current state-of-the-art and recommended applications in biotechnology, Appl. Microbiol. Biotechnol. 86 (2010) 41–49.
[19] H. Cho, J. Mu, J.K. Kim, J.L. Thorvaldsen, Q. Chu, E.B. Crenshaw, K.H. Kaestner, M.S. Bartolomei, G.I. Shulman, M.J. Birnbaum, Insulin resistance and a diabetes mellitus-like syndrome in mice lacking the protein kinase Akt2 (PKBβ), Science 292 (2001) 1728–1731.
[20] U.K. Laemmli, Cleavage of structural proteins during the assembly of the head of bacteriophage T4, Nature 227 (1970) 680–685.
[21] H.S. Wang, F.Z. Wang, X.F. Zhu, Y.C. Yan, X.H. Yu, P.X. Jiang, X.H. Xing, Biosynthesis and characterization of violacein deoxyviolaceiri and

oxyviolacein in heterologous host, and their antimicrobial activities, Biochem. Eng. J. 67 (2012) 148–155.
[22] G.I. Frost, R. Stern, A microtiter-based assay for hyaluronidase activity not requiring specialized reagents, Anal. Biochem. 251 (1997) 263–269.
[23] S. Shulga-Morskoy, B. Rich, Bioactive IL7-diphtheria fusion toxin secreted by mammalian cells, Protein Eng. Des. Sel. 18 (2005) 25–31.
[24] E. Grabenhorst, P. Schlenke, S. Pohl, M. Nimtz, H.S. Conradt, Genetic engineering of recombinant glycoproteins and the glycosylation pathway in mammalian host cells, Glycoconj. J. 16 (1999) 81–97.
[25] H.M. Kinnunen, R.J. Mrsny, Improving the outcomes of biopharmaceutical delivery via the subcutaneous route by understanding the chemical, physical and physiological properties of the subcutaneous injection site, J. Control. Release 182 (2014) 22–32.
[26] D.B. Muchmore, D.E. Vaughn, Review of the mechanism of action and clinical efficacy of recombinant human hyaluronidase coadministration with current prandial insulin formulations, J. Diabetes Sci. Technol. 4 (2010) 419–428.
[27] C.J. Porter, S.A. Charman, Lymphatic transport of proteins after subcutaneous administration, J. Pharm. Sci. 89 (2000) 297–310.
[28] K.S. Girish, K. Kemparaju, The magic glue hyaluronan and its eraser hyaluronidase: a biological overview, Life Sci. 80 (2007) 1921–1943.
[29] S. Misbah, M.H. Sturzenegger, M. Borte, R.S. Shapiro, R.L. Wasserman, M. Berger, H.D. Ochs, Subcutaneous immunoglobulin: opportunities and outlook, Clin. Exp. Immunol. 158 (2009) 51–59.